An Investigation of Natural Ventilated Roofs by means of Computational Fluid Dynamics

Jompob Waewsak
Renewable Energy System Research and Demonstration Center (RESRDeC)
Physics Department, Faculty of Science, Thaksin University, Phatthalung, 93110, Thailand
Tel: 66-74 693995, Fax: 66-74 693995, E-mail: jompob@tsu.ac.th
Rangsit Sarachitti
Quantitative Science Department, Faculty of Arts and Sciences
Dhurakijpundit University, Bangkok, 10210, Thailand

Abstract

This paper presents an investigation of natural ventilation within the bioclimatic roof (BCR) and the roof solar collector (RSC). The objective of this study is to apply computational fluid dynamics (CFD) in three dimensions. This is based upon the standard $k-\varepsilon$ turbulence model in order to study the characteristics of air in the gap, in terms of temperature and velocity as well as average h_c of both roofs. The finite volume method is used to solve the Navier-Stokes equations. Simulations were carried out by applying the boundary conditions based on experimental data in winter (December 1999) and summer (March 2000) conditions of Thailand. The predicted data by the CFD program was validated against the experimental data and good agreement was achieved. Comparison results of both roofs were made and the findings are presented in this paper.

Keywords: natural ventilation roofs, computational fluid dynamics, bioclimatic roof, solar collector

1. Introduction

There are two modeling approaches related to building energy simulation i.e. zonal networks and computational fluid dynamics (CFD) [1-2]. Although well adapted for building energy application, the zonal network method is limited because the momentum effects are neglected [2]. As a result of low resolution, local surface convection heat transfer is poorly represented. To overcome these limitations, it is imperative to conflate CFD and building simulation. There were various research works worldwide on building simulation using a CFD technique [3-5], especially that involved directly the roof [6]. However, research work on CFD in building simulation in Thailand is rather rare. Some research studies in this area in Thailand using the CFD technique are presented in [7-9].

The roof is the most important part of a building envelope because it is largely and continuously exposed to the sky. Solar induced natural ventilation can be applied by a solar chimney when the openings are appropriately installed. Normally, roof tiles are isolated from the occupied space. Therefore, it can be heated as much as possible by absorbing incident solar radiation. Air in the gap simply flows to the top of the chimney by the buoyancy effect. The stagnant room air is then extracted, providing natural ventilation and also reducing heat gain passing through the roof [10].

Over the years, the bioclimatic roof (BCR) and the roof solar collector (RSC) have been promoted to provide natural ventilation in buildings design. These roofs emphasize thermal and ventilation performance. During the day the BCR and the RSC act as a solar chimney, which also helps in ventilation. The BCR permits the use of indirect daylight, while during the night, it acts as a roof radiator. The BCR consists of a combination of both concrete and transparent tiles at the top, a gap to allow airflow in the middle, and another combination of gypsum with aluminum foil board and translucent sheets at the bottom. On the other hand, the RSC consists only of concrete tiles at the top, a gap to allow airflow in the middle, and gypsum board at the bottom. The descriptions of the RSC and

the BCR are shown in Fig. 1. The BCR and the RSC were integrated into the school solar house. The experiments were conducted and executed under the tropical climate of Thailand in order to investigate their thermal and lighting performances.

The performance of both BCR and RSC were extensively investigated based on field-testing and the results were clearly presented in [10-13]. The previous studies of natural heat convection within the BCR and the RSC aimed at predicting the airflow rate, and also applied an empirical model introduced by Bansal [14]. Recently, it has been shown that the heat transfer coefficient of the RSC has been promoted based on its experiments and correlations. [15-16].

However, the characteristics of airflow and the temperature in the air gap of the BCR and RSC have never been carried out. Although the use of high precision equipment for real-time visualization and in situ monitoring of the airflow in both roofs seem to be complicated, the main constraint is the cost. Consequently, the objective of this study is to investigate the natural ventilation within the BCR and the RSC, which are later simplified to be partially glazed and unglazed inclined open-ended rectangular channels by means of CFD simulation [17].

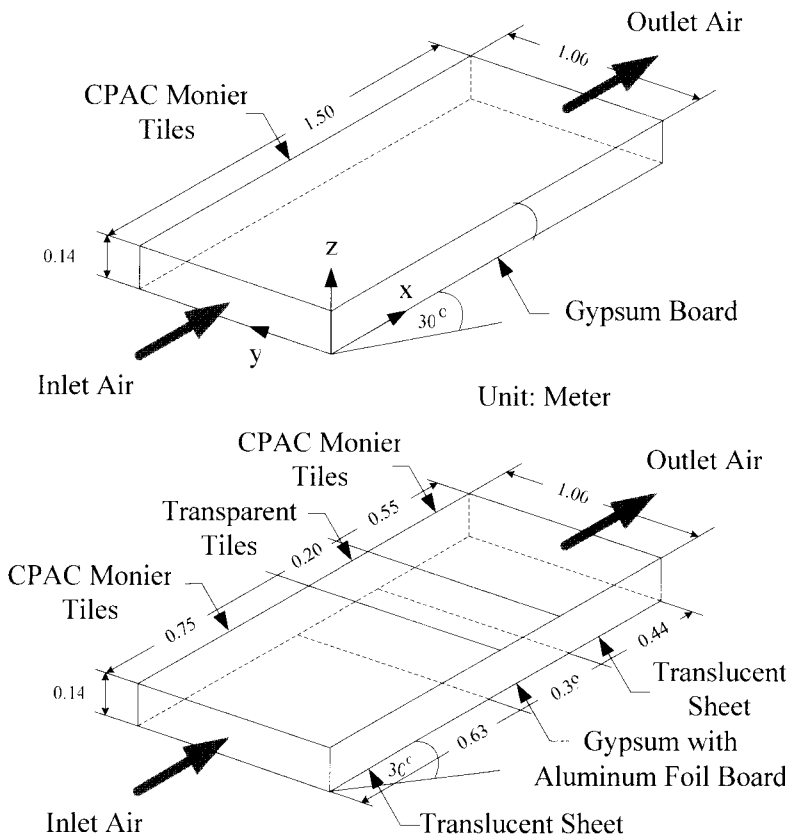

Fig 1. Description of the RSC (upper) and the BCR (lower).

2. Assumptions and Simulation Technique

In order to study the natural heat convection within the BCR and the RSC, the following assumptions are formulated:

- The BCR and the RSC were considered as partially glazed and unglazed inclined open-ended rectangular channels.
- Heat is transferred in three dimensions under the steady state condition.
- Air in the gap is considered as a non-radiative gas with no heat generation.
- The airflow is turbulent.
- The radiation exchange between the upper and lower surfaces of the gap is neglected.

By accepting the Boussinesq approximation, all thermal properties of air except density are constant and the buoyant flow could be expressed in terms of a temperature gradient rather than represented in terms of a density gradient.

2.1 Governing Equations

The Navier-Stokes equations were used to describe the motion of fluid. The flow field can be described by the conservation equations of mass, momentum components and thermal energy. By applying the above assumptions, the governing equations can be written in vector form as shown in the following equations.

The continuity equation :

$$\nabla \vec{V} = 0$$

The momentum equation in x, y and z component :

$$\rho(\vec{V} \cdot \nabla \vec{V}) = -\nabla \vec{P} + \mu(\nabla^2 \vec{V}) - \rho g_i, \; i = x, y, z$$

The energy equation :

$$\rho c_p(\vec{V} \cdot \nabla T) = k(\nabla^2 T)$$

Where $\vec{V}$ is the velocity vector, p is the pressure, μ is the fluid viscosity, k is the thermal conductivity, ρ is the air density, c_p is the specific heat capacity, g is the Earth's gravitational acceleration and T is the temperature in Kelvin.

Although the new model of turbulence was proposed in [18], the standard $k-\varepsilon$ turbulence model was still suitable and convenient [19-22]. In this study turbulence is accounted for by the standard version $k-\varepsilon$ model together with appropriate treatments for the conditions at the wall boundaries. All equations were solved simultaneously by using the finite volume method. The boundary conditions of the BCR and the RSC are presented in the next section.

2.2 Boundary Conditions

The discretization of the BCR and the RSC are an unconstruction grid, in the range of $0.02\,m$. The finite element method was used to construct the grid. Boundary conditions of both roofs are considered as a constant wall temperature based upon the experimental results [13]. For the singular points, the boundary singularity was applied for simplicity [23]. The inlet air velocity of both roofs is at normal speed and also based on results from the experiments in the summer and winter conditions of Thailand. The thermal boundary conditions of the RSC and BCR are presented in Fig. 2, where T_{cs} and T_{cw} stand for the temperature of CPAC Monier tiles in summer and in winter respectively, T_{gs} and T_{gw} stand for the temperature of gypsum board in summer and in winter respectively, T_{ss} and T_{sw} stand for the temperature at both sides of the BCR and the RSC in summer and in winter respectively, V_s and V_w stand for the normal inlet air speed in summer and winter respectively, T_{tps} and T_{tpw} stand for the temperature of transparent tiles in summer and in winter respectively, T_{gfs} and T_{gfw} stand for the temperature of translucent sheets in the summer and in winter respectively. T_{is} and T_{iw} stand for the inlet air temperature in summer and winter of the BCR and the RSC, respectively.

As mentioned earlier, these thermal boundary conditions were obtained from the experiments conducted during winter (December 1999) and summer (March 2000) in Thailand.

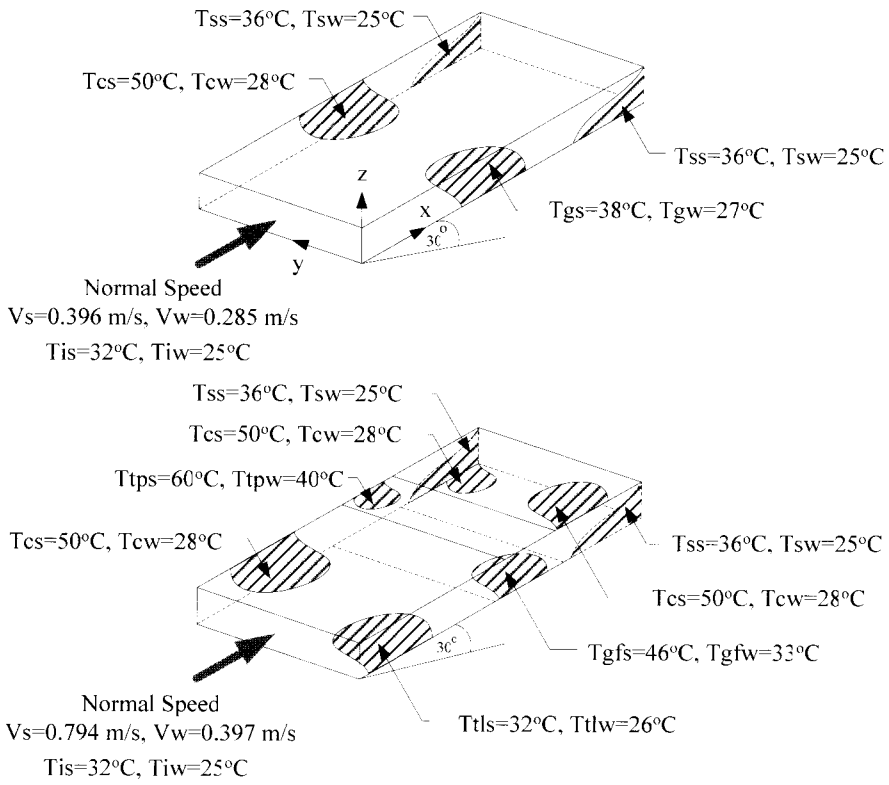

Fig. 2. Thermal boundary conditions of the RSC (upper) and the BCR (lower).

Generally, the inlet air velocity can be considered as the Cartesian velocity, the velocity profile, the uniform flow, zero velocity, pressure gradient, relative pressure, etc. With reference to this study, the inlet air velocity of both roofs were considered as the uniform speed due to the speed of inlet air which was obtained from the measurement. We supposed that the direction of the inlet air was parallel to the horizontal plane for simplicity. The simulation results were obtained by running the CFX computer software [24] with these thermal boundary conditions. The average convective heat transfer coefficients of the upper and lower surface of the air gap were found based on the Newton cooling law of heat conduction [25].

3. Results and Discussion

The temperature distribution of air in the air gap of RSC in summer and winter is based on the standard $k-\varepsilon$ turbulence model of CFD prediction as shown in Fig. 3 and Fig. 4. The velocity profile within the RSC in the summer and winter are shown in Fig. 5 and Fig. 6. The velocity vector within the RSC in the summer and winter are shown in Fig. 7 and Fig. 8, respectively.

For the BCR, the temperature distribution of air in the air gap for summer and winter from the simulation are shown in Fig. 9 and Fig. 10.The velocity profile in the summer and winter are shown in Fig. 11 and Fig. 12. The velocity vector within the BCR in the summer and winter are shown in Fig.13 and Fig.14, respectively.

The boundary condition of both RSC and BCR were defined as the constant wall temperature. The maximum temperature occurred during summer and was found to be 60°C for the BCR and 50°C for the RSC. Simulation results revealed that the temperature gradient was near the upper surface of the air gap within the RSC as shown in Fig.3 and Fig.4. The temperature difference clearly represents the greenhouse

effect as shown in Fig. 9 and Fig. 10. Due to the thermal radiation being neglected in the simulation; the heat might be transferred to air by natural convection only. Hence, the magnitude of the temperature gradient is displayed along the surface of roof tiles only. The temperature of air in the gap was expected to be increased if the thermal radiation between the upper surface and the lower surface of both roofs were taken into consideration in the simulation.

However, this indicated that both RSC and BCR could reduce heat gain of the occupied space. The significant temperature gradient is display near the upper surface of both roofs only.

The temperature at the mid-plane of the air gap (See Fig. 3.), from the measurement and simulation, were compared for both roofs for validation. Results in winter (December 1999) and summer (March 2000) are shown in Table 1 and Table 2, respectively.

Table 1. Measured and simulated temperature at mid-plane in degrees Celsius of both roofs in winter (December 1999).

Mid-Plane Temperature	RSC		BCR	
	M	S	M	S
T1	25.00	25.00	26.50	25.72
T2	25.00	25.32	28.00	27.37
T3	25.00	25.32	30.00	28.16
T4	25.00	25.76	28.00	27.37
T5	25.00	25.76	27.50	27.37

Note: M = measured and S = simulated

Table 2. Measured and simulated temperature at mid-plane in degrees Celsius of both roofs in summer (March 2000).

Mid-Plane Temperature	RSC		BCR	
	M	S	M	S
T1	36.00	33.89	35.20	32.00
T2	37.00	36.74	37.80	33.47
T3	37.50	36.74	40.00	39.37
T4	36.80	35.79	38.00	36.42
T5	36.00	35.79	37.70	34.99

Note: M = measured and S = simulated

The heat transfer coefficient of the upper and lower surfaces of the air gap can be computed by using a simple Newton's law of cooling. Results are shown in Table 3. The findings reveal that the average convective heat transfer coefficients of the upper and lower surfaces of the air gap were in the range of 1.98-3.69 $W/m^2 \cdot K$ for the RSC and 2.39-9.22 $W/(m^2 \cdot K)$ for the BCR. From the results, we can conclude that the BCR has good performance because it has higher thermal and convective heat transfer coefficients as compared to the RSC, indicating that heat accumulation in the roof gap is reduced.

The average predicted outlet air velocity of the RSC and the BCR in winter (December 1999) and summer (March 2000) are presented in Table 4 and Table 5, respectively. The effect of boundary conditions at the inlet of the RSC for summer and winter are shown in Fig. 5 and Fig.6., while Fig. 11 and Fig. 12 show the effect of inlet air, considered to be normal speed of the BCR in summer and winter, respectively.

Table 3. The average convective heat transfer coefficients (h_c) of the upper and lower surfaces of the air gap [$W/(m^2 \cdot K)$].

Roof Design	Summer		Winter	
	Upper	Lower	Upper	Lower
RSC	3.03	3.69	1.98	2.76
BCR	3.97	9.22	2.39	4.50

Table 4. Average predicted and measured outlet air velocity [m/s] of RSC in summer and winter.

Design	Measured	Predicted	%Error
Summer	0.45	0.47	-4.26
Winter	0.31	0.33	-6.45

Table 5. Average predicted and measured outlet air velocity [m/s] of BCR in summer and winter.

Design	Measured	Predicted	%Error
Summer	0.69	0.80	-13.75
Winter	0.41	0.46	-12.19

4. Conclusion

Temperature and velocity profiles in the air gap of both RSC and BCR were investigated by means of a computational fluid dynamics (CFD) technique. Results have been presented in this paper. Heat transfer coefficients and outlet air velocities were the output of the simulation. The simulation was validated against the experimental results and the difference was insignificant. However, from the experimental and numerical studies of the RSC and the BCR,

it can be suggested that the building envelopes should be designed to provide maximum ventilation by the combination of solar chimney (stack effect) and wind induced natural ventilation. Not only that, the performance of the BCR could be enhanced by increasing the transparent tiles for increasing both daylight and maximizing natural ventilation.

5. Acknowledgement

The authors gratefully acknowledge Mr. Auttapol Golaka, Joint Graduate School of Energy and Environment, KMUTT for his kind help in Computational Fluid Dynamics analysis.

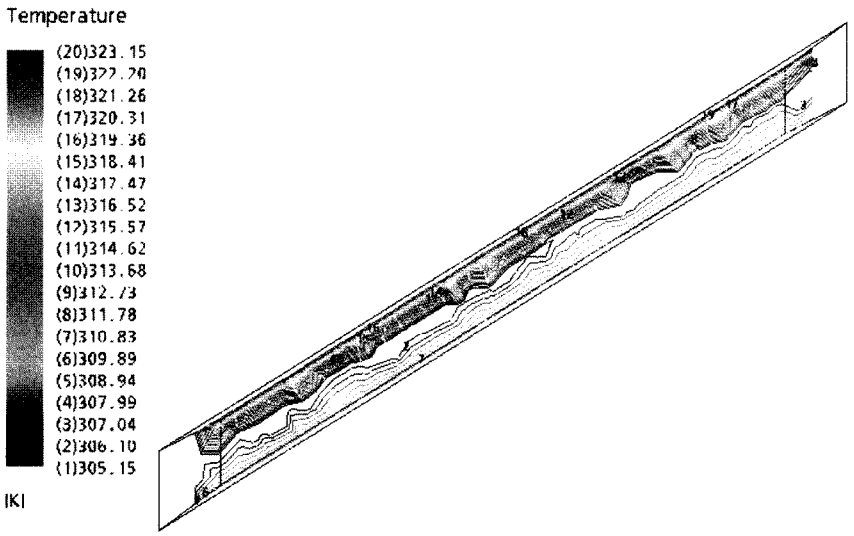

Fig. 3. Mid plane temperature contour in the air gap of the RSC in summer (March 2000), T_{cs} =50°C, T_{ss} =36 °C, T_{gs} =38°C, T_{is} =32°C and grid size of 0.02 m .

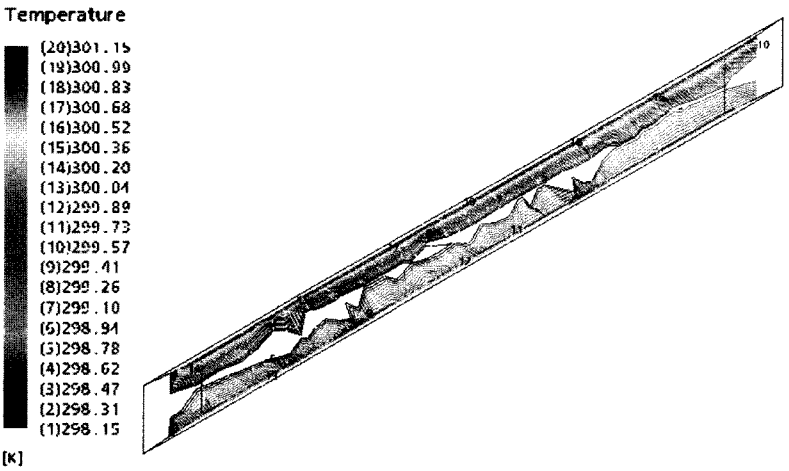

Fig. 4. Mid-plane temperature contour in the air gap of the RSC in winter (December 1999), T_{cw}=28°C, T_{sw} =25°C, T_{gw}=27°C, T_{iw} =25°C and grid size of 0.02 m .

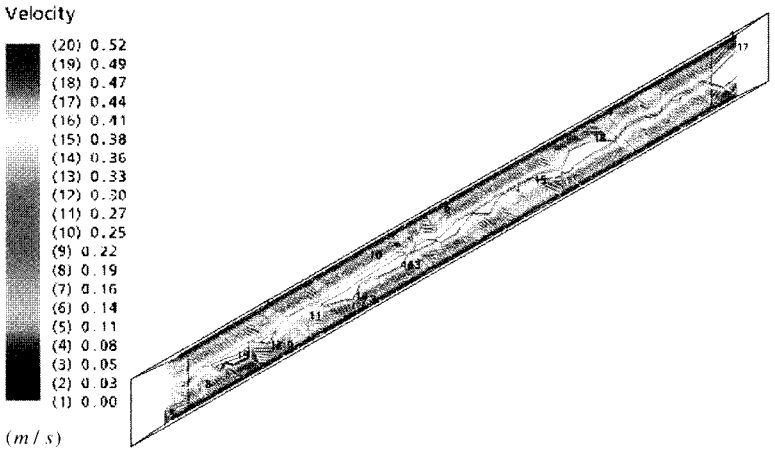

Fig. 5. Mid-plane velocity contour in the air gap of the RSC in summer (March 2000), V_S=0.396 m/s and grid size of 0.02 m.

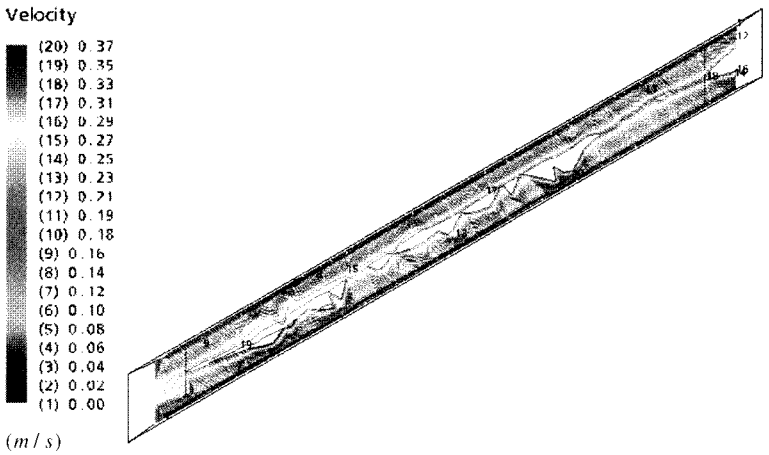

Fig. 6. Mid-plane velocity contour in the air gap of the RSC in winter (December 1999), V_W=0.285 m/s and grid size of 0.02 m.

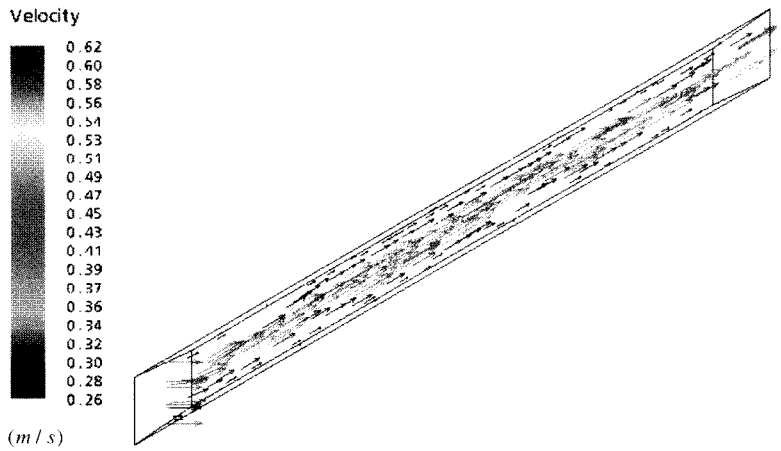

Fig. 7 Velocity vector in the air gap of the RSC in summer (March 2000), V_S=0.396 m/s and grid size of 0.02 m.

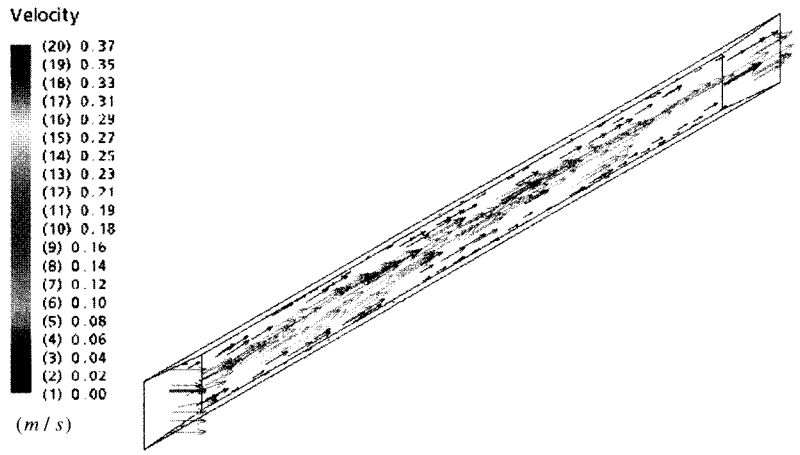

Fig. 8. Velocity vector in the air gap of the RSC in winter (December 1999), V_W=0.285 m/s and grid size of 0.02 m.

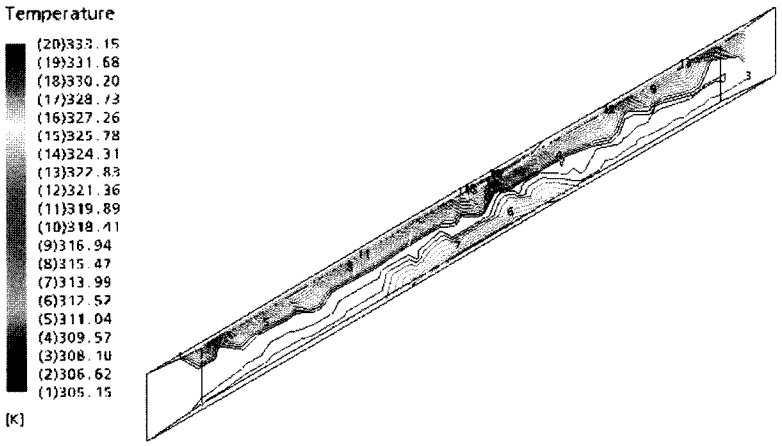

Fig. 9. Mid-plane temperature contour in the air gap of the BCR in summer (March 2000), T_{cs} =50°C, T_{tps} =60°C, T_{gfs} =46°C, T_{tls} =32°C, T_{ss} =36 °C and grid size of 0.02 m .

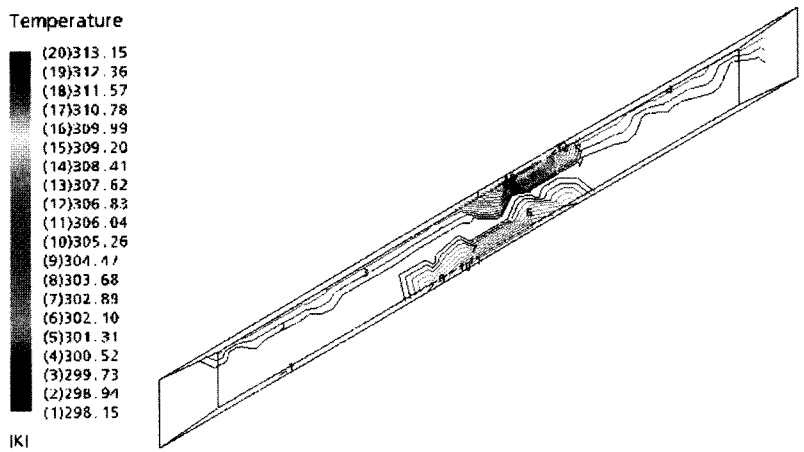

Fig. 10. Mid-plane temperature contour in the air gap of the BCR in winter (December 1999), T_{cw} =28°C, T_{tpw} =40°C, T_{gfw} =33°C, T_{tlw} =26°C, T_{sw} =25°C and grid size of 0.02 m .

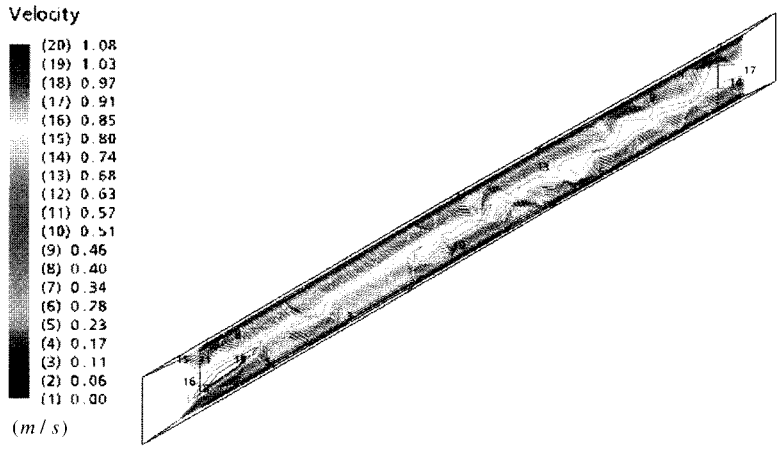

Fig. 11. Mid-plane velocity contour in the air gap of the BCR in summer (March 2000), $V_S = 0.794\ m/s$ and grid size of $0.02\,m$.

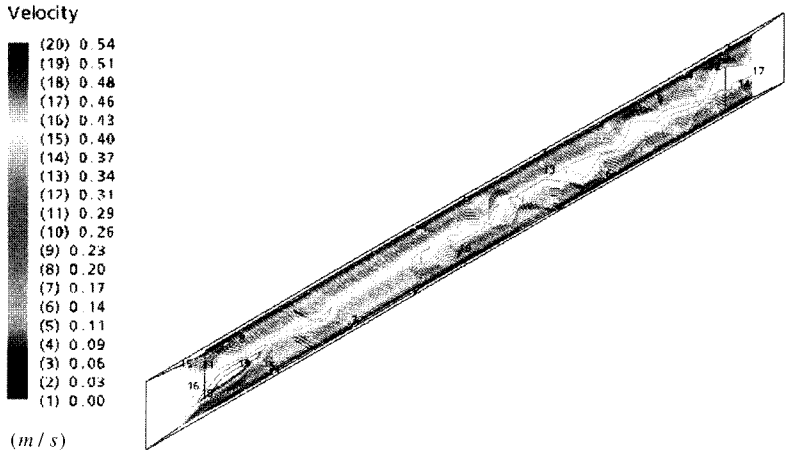

Fig. 12. Mid-plane velocity contour in the air gap of the BCR in winter (December 1999), $V_W = 0.397\,m/s$ and grid size of $0.02\,m$.

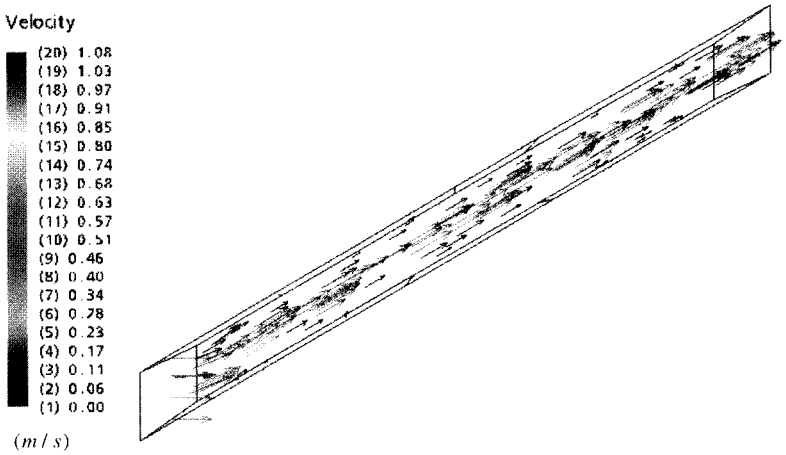

Fig. 13. Velocity vector in the air gap of the BCR in winter summer (March 2000), $V_S = 0.794\ m/s$ and grid size of $0.02\,m$.

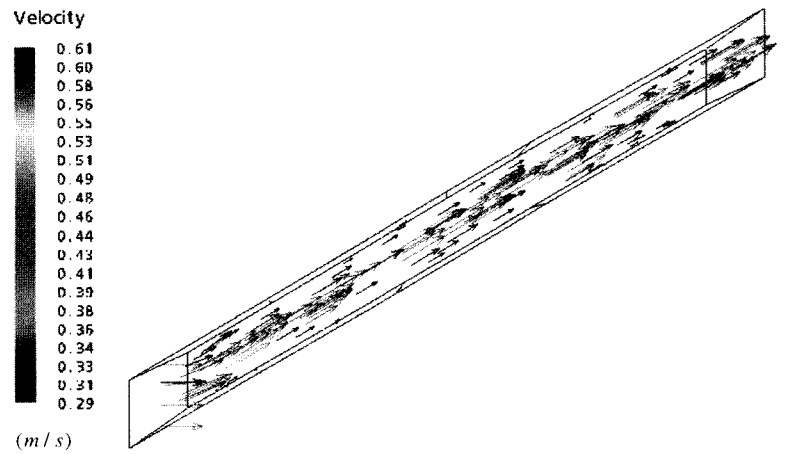

Fig. 14. Velocity vector in the air gap of the BCR in winter (December 1999), $V_W = 0.397\,m/s$ and grid size of $0.02\,m$.

6. References

[1] Wurtz, E. Nataf, J. M. and Winkelmann, F, Two and Three Dimensional Natural and Mixed Convection Simulation using Modular Zonal Models in Buildings, *International Journal of Heat and Mass Transfer* 42, pp.923-940, 1999.

[2] Bartak, M., Morrison, I. B., Clarke, J. A. Denev, J. Drkal, F. and Lain, M., Integrating CFD and Building Simulation, *Building and Environment* 37, pp.865-871, 2002.

[3] Clifford, M. J., Everitti, P. G., Clarke, R. and Riffat, S. B., Using Computational Fluid Dynamics as a Design Tool for Naturally Ventilated Buildings, *Building and Environment* 32, pp.305-312, 1997.

[4] Gan, G. and Riffat, S. B., A Numerical Study of Solar Chimney of Natural Ventilation of Buildings with Heat

Recovery, *Applied Thermal Engineering* 18, pp.1171-1187, 1998.

[5] Cezar, O. R. Negrao, Integration of Computational Fluid Dynamics with Building Thermal and Mass Flow Simulation, *Energy and Buildings* 27, pp. 155-165, 1998.

[6] Kindangen, J., Krauss, G. and Depecker, P., Effects of Roof Shapes on Air Induced Motion inside Buildings, *Building and Environment* 32, pp.1-11, 1997.

[7] http://www.acat.or.th/library/INDEX.HTM

[8] Tantasavasdi, C., Srebric, J. and Chen, Q., Natural Ventilation Design for Houses in Thailand, *Energy and Buildings* 33, pp. 815-824, 2001.

[9] Chungloo, S., Limmeechokchai, B. and Chungpaibulpatana, The Numerical Investigation of an Integrated Passive Cooling System: The Case Study of Thailand, *The 1st International Conference on Sustainable Energy and Green Architecture*, 8-10 October 2003, Bangkok, Thailand.

[10] Hirunlabh, J., Wachirapuwadon, S., Pratinthong, N. and Khedari, J., New Configuration of a Roof Solar Collector Maximizing Natural Ventilation, *Building and Environment* 4, pp.1-9, 2000.

[11] Khedari, J., Mansirisub, W., Chaima, S., Pratinthong, N. and Hirunlabh, J., Field Measurements of Performance of Roof Solar Collector, *Energy and Buildings* 31, pp. 171-178, 2000.

[12] Khedari, J., Mansirisub, W., Chaima, S., Pratinthong, N. and Hirunlabh, J., Field Measurements of Performance of Roof Solar Collector, *Energy and Buildings* 31, pp.171-178, 2000.

[13] Waewsak, J., Hirunlabh, J., Khedari, J. and U. C. Shin, Performance Evaluation of the BSRC Multi-Purpose Bio-Climatic Roof, *Building and Environment* 38, pp.1297-1302, 2003.

[14] Bansal, N. K., Mathur, R. and Bhandari, M. S., Solar Chimney for Enhanced Stack Ventilation, *Building and Environment* 28, pp.373-377, 1992.

[15] Khedari, J., Yimsmerjit, P. and Hirunlabh, J., Experimental Investigation of Free Convection in Open-Ended Inclined Rectangular Channel with Upper Hot Plate, *Building and Environment* 37, pp.455-459, 2002.

[16] Puangsombat, W., Hirunlabh, J. and Khedari, J., Experimental Investigation of Free Convection Produced by a Heated Top Plate in an Open Ended Inclined Rectangular Channel with Radiant Barrier, *The 1st International Conference on Sustainable Energy and Green Architecture*, 8-10 October 2003, Bangkok, Thailand.

[17] Chung, T. G., Computational Fluid Dynamics, *Cambridge University Press* ,2002.

[18] Chantasaro, E. and Chantasaro, V., On the New Concept of Turbulence Modeling, *The 7th Annual National Symposium on Computational Science and Engineering*, 24-26 March 2003, Bangkok, Thailand.

[19] Launder B. E. and Spalding, D. B., The Numerical Computation of Turbulent Flows, *Computer Methods in Applied Mechanics and Engineering* 3, pp.269-289, 1974.

[20] Chen, Q., Xu, W. A., A Zero-Equation Turbulence Model for Indoor Airflow Simulation, *Energy and Buildings* 28, pp. 137-144, 1998.

[21] Awbi, H. B., Calculation of Convective Heat Transfer Coefficient of Room Surface for Natural Convection, *Energy and Buildings* 28, pp.219-227, 1998.

[22] Sukjit, E., Juntasaro, V., Utthayopas, P. and Juntasaro, E., Numerical Simulation of Turbulent Flow in Three-Dimensional Space, *The 7th Annual National Symposium on Computational Science and Engineering*, 24-26 March 2003, Bangkok, Thailand.

[23] Lam, C. Y., Applied Numerical Methods for Partial Differential Equations, Prentice Hall, 1994.

[24] www.ansys.com/cfx.

[25] Incropera, F. P. and DeWitt, D. P., Introduction to Heat Transfer, John Wiley&Sons, 1996.